Eur. J. Mineral.
2014, **26**, 179–188
Published online February 2014

Hydrothermal transformations of triphylite from the Nanping No. 31 pegmatite dyke, southeastern China

CAN RAO[1,*], RU CHENG WANG[2], FRÉDÉRIC HATERT[3] and MAXIME BAIJOT[3]

[1] Department of Earth Sciences, Zhejiang University, Hangzhou 310027, China
*Corresponding author, e-mail: canrao@zju.edu.cn
[2] State Key Laboratory for Mineral Deposits Research, School of Earth Sciences and Engineering, Nanjing University, Nanjing 210093, China
[3] Laboratoire de Minéralogie, Université de Liège, B18, 4000 Liège, Belgium

Abstract: The mineralogy of triphylite and associated phosphates was investigated in the Nanping No. 31 pegmatite, southeastern China. Two types of triphylite were distinguished, based on their petrological features and chemical compositions. Triphylite-I occurs as small granular aggregates in fine grained white mica from zones III and IV, whereas triphylite-II occurs as veinlets or aggregates in the fractures and/or on the rims of primary montebrasite from zone IV. Various hydrothermal transformations were observed in both types of triphylite. Triphylite-I successively transformed to lazulite, wagnerite, fluorarrojadite-(BaNa) and fluorapatite, suggesting successive replacement processes during Mg-rich, Na-rich, and Ca-rich hydrothermal stages. Triphylite-II is mainly replaced by fluorapatite, anapaite, and ludlamite; these replacement processes result from cationic exchanges in combination with hydration, due to the presence of Ca-bearing fluids.

Key-words: triphylite, wagnerite, fluorarrojadite-(BaNa), lazulite, anapaite, ludlamite, Nanping No. 31 pegmatite, China.

1. Introduction

Triphylite, $Li(Fe,Mn)^{2+}PO_4$, is a common primary mineral in rare-element granitic pegmatites (Černý, 1991; Černý & Ercit, 2005). Its transformation by hydrothermal fluids induces the formation of secondary phosphate minerals of the ferrisicklerite $[Li_{1-x}(Fe^{3+},Mn^{2+})PO_4]$ – heterosite $[(Fe^{3+},Mn^{3+})PO_4]$ series; this transformation process is known as the Quensel-Mason sequence (Quensel, 1937; Mason, 1941). The mineralogy and metasomatic alteration of triphylite in pegmatites have been extensively described in the literature (Shigley & Brown, 1985; Fransolet *et al*., 1986; Keller & Von Knorring, 1989; Roda *et al*., 2004; Nizamoff *et al*., 2006; Vignola *et al*. 2008; Hatert *et al*., 2011; Vignola *et al*., 2011; Baijot *et al*., 2012). The past decades have seen an increasing number of studies related to triphylite-type phosphates, since these compounds show electrochemical properties of great interest in the development of cathode material for lithium batteries (*e.g*., Padhi *et al*., 1997; Dokko *et al*., 2007; Zhao *et al*., 2010). For this reason, the petrographic features of natural triphylite are of peculiar significance.

The Nanping No. 31 pegmatite is a rare-element, well mineralized pegmatite from southeast China (Yang *et al*., 1987; Rao *et al*., 2009). In this pegmatite, triphylite occurs in zones III (Na-metasomatic unit) and IV (intermediate unit), and two types of triphylite were distinguished according to their petrographic features and chemical compositions (Trp-I and Trp-II). Interestingly, both types of triphylite were hydrothermally transformed, forming various secondary phosphates such as lazulite, wagnerite, fluorarrojadite-(BaNa), fluorapatite, anapaite and ludlamite. In this paper, we present the mineralogical features of these two generations of triphylite and of the secondary phosphates; these data will shed some light on the formation and transformation processes that affected triphylite in the Nanping No. 31 pegmatite.

2. Geological setting and petrological background

The Nanping pegmatite was first described as a Nb-Ta-bearing pegmatite by Li *et al*. (1983). It is located in the southeast margin of a Caledonian folded belt, in the northwest Fujian Province, southeastern China. In this pegmatite district occur about 500 pegmatites dykes, outcropping on an area reaching approximately 250 km^2. Pegmatites generally form lenticular bodies with a general N-NE orientation, intruded in Meso- and Neo-Proterozoic schists and granulites of Xiafeng fabric. These schists and granulites are intruded by Hercynian and Yanshanian (Jurassic) granites, and are partially covered by discordant Jurassic and Permian sediments (Fig. 1a).

DOI: 10.1127/0935-1221/2014/0026-2357
0935-1221/14/0026-2357 $ 4.50

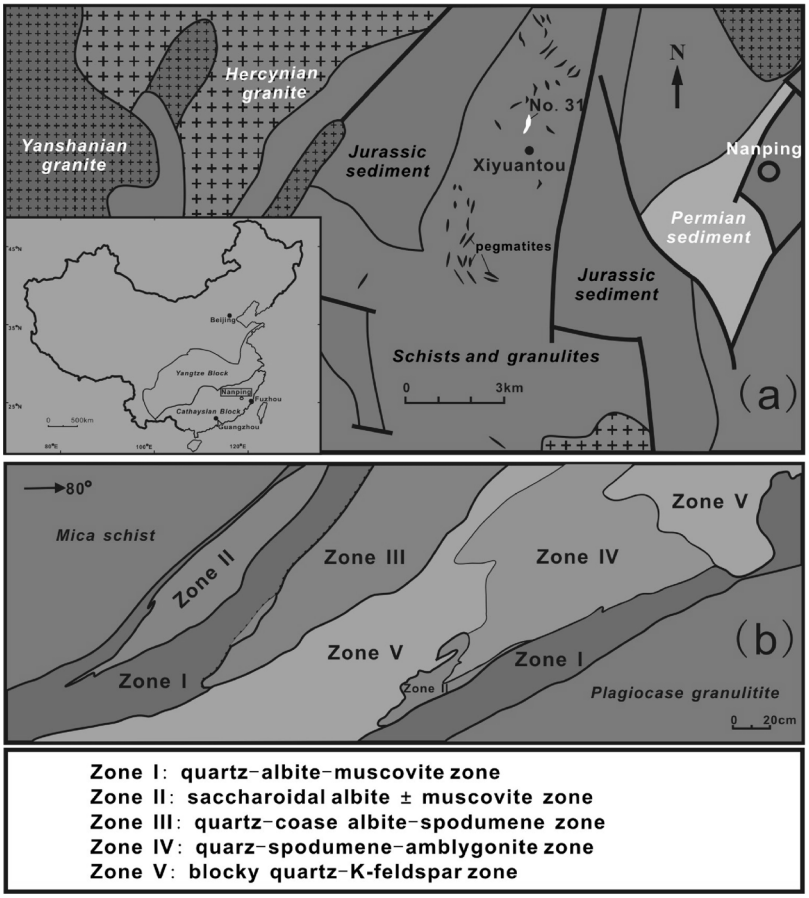

Fig. 1. (a) Simplified geological map of the Nanping pegmatite district; (b) internal textural zones observed at the level of 515 m from the No.31 granitic pegmatite dyke (modified after Yang *et al*., 1987). Zone I = wall zone; zone II = saccharoidal replacement unit; zone III = Na-metasomatic unit; zone IV = intermediate unit; zone V = quartz core and core-margin zone.

The occurrence, shape and distribution of pegmatite dykes were strongly controlled by deformation processes. Based on their different degrees of fractionation, Yang *et al*. (1987) divided these pegmatites into four groups: muscovite–orthoclase–albite (tabular) pegmatite (type I); muscovite–albite–orthoclase pegmatite (type II); muscovite–orthoclase–albite (fine grained) pegmatite (type III), and muscovite–albite–spodumene pegmatite (type IV). The Nanping No. 31 pegmatite, in which the samples investigated in this paper were collected, is a type IV pegmatite. It constitutes one of the most highly differentiated and well-mineralized pegmatites in the Nanping pegmatite district; in the past several decades, it was mainly mined for Nb-Ta-Sn-oxides. This pegmatite belongs to the rare-element class, complex type, spodumene sub-type, according to the international classification (Černý, 1991; Černý & Ercit, 2005). It shows a LCT (lithium, cesium, tantalum) geochemical signature.

The Nanping No. 31 pegmatite is located in the Xiyuantou area, 8 km west of the city of Nanping. It consists of lenticular bodies with a predominant N-NE orientation, which are steeply intruded into schists and granulites (Fig. 1a). The No. 31 pegmatite is 5 to 6 m in width, 90 m in depth, and 300–600 m in length. Figure 1b shows the different zones observed in the open pit at 515 m level, which comprises roughly five discontinuous zones from the outermost zone inward (Yang *et al*., 1987). Zone I (wall zone, according to the international nomenclature; see Simmons *et al*., 2003 and London, 2008) is mainly composed of medium-grained quartz, muscovite and fine-grained albite. Other minerals include cassiterite, columbite–tantalite-group minerals, zircon, beryl, hurlbutite, phenakite, fluorapatite, and strontiohurlbutite (Rao *et al*., 2013). Zone II (saccharoidal replacement unit) typically contains saccharoidal albite and greenish muscovite. This zone can be further subdivided into facies IIa (saccharoidal albite $>$ 90 vol. %, greenish muscovite $<$ 10 vol. %) and facies IIb (60 vol. % greenish muscovite with 10 vol. % quartz and 30 vol. % albite). Black minerals such as cassiterite, columbite–tantalite-group minerals, wodginite-group minerals and tapiolite-(Fe), are mainly concentrated at the boundary between the two facies. Other accessory minerals are beryl, phenakite, hydroxyherderite, hurlbutite, euclase, strontiohurlbutite and fluorapatite. Zone III (Na-metasomatic unit) is characterized by platy crystals of albite (variety ''cleavelandite''), coarse quartz and spodumene. Columbite–tantalite-group minerals, wodginite-group minerals, tapiolite-(Fe), microlite, zircon, cassiterite, fluorapatite, amblygonite–montebrasite and beryl

are present as accessory minerals. Zone IV (intermediate unit) mainly contains coarse-grained quartz, massive spodumene, and montebrasite crystals. Accessory minerals mainly include columbite-group minerals, wodginite-group minerals, tapiolite-(Fe), microlite-group minerals, beryl, cassiterite, pollucite, lazulite and strontiohurlbutite. Massive montebrasite crystals in this zone are frequently altered to secondary phosphate minerals: palermoite, bertossaite, kulanite and hydroxylapatite (Yang *et al*., 1995). Finally, most of the spodumene crystals in zones III and IV were completely altered to fine-grained white mica assemblages (Rao *et al*., 2012). Zone V (quartz core and core-margin zone) at the pegmatite core consists of blocky quartz and K-feldspar; accessory minerals are very rare.

3. Sampling and analytical methods

The rock samples investigated in the present study were collected on the dumps from the mine opening at the 515 m level, in the Nanping No. 31 pegmatite dyke. The zones from which the samples were extracted were identified on the basis of the observed mineral assemblages.

Chemical compositions of phosphate minerals were determined with a JEOL JXA-8100M electron microprobe using wavelength-dispersion spectrometry (WDS) in the State Key Laboratory for Mineral Deposits Research at Nanjing University. The microprobe was operated at a beam current of 20 nA, an accelerating potential of 15 kV, and a beam 1 μm in diameter for all elements. Element peaks and backgrounds were measured with counting times of 10 s on the peak and 5 s on the background. The following standards were used: albite (Si), hornblende (Na, K, Mg, Al, Ca, and Fe), fluorapatite (P and F), $MnTiO_4$ (Mn), synthetic $Ba_3(PO_4)_2$ (Ba), synthetic $SrSO_4$ (Sr). A ZAF programme was used for all data reduction.

4. Mineralogy of triphylite assemblages

4.1. Petrography and chemical composition of triphylite

In the Nanping No. 31 pegmatite, triphylite was found in zones III and IV. On the basis of petrological textures and chemical compositions, two different types of triphylite were distinguished. Triphylite-I (noted Trp-1) occurs as small rounded grains from 80 to 200 μm diameter, included in fine-grained white mica from zones III and IV (Fig. 2). Associated minerals include lazulite, wagnerite, fluorarrojadite-(BaNa), palermoite, and fluorapatite. Triphylite-II (noted Trp-2) is the most common occurrence of triphylite in the Nanping No. 31 pegmatite. It forms fine-grained intergrowths with muscovite, located at the rims of primary montebrasite grains from zone IV (Fig. 3a), or forming veinlets within fractures crosscutting this mineral (Fig. 3b). The veinlets are up to 1 mm wide and several cm in length. Fine-grained muscovite, quartz,

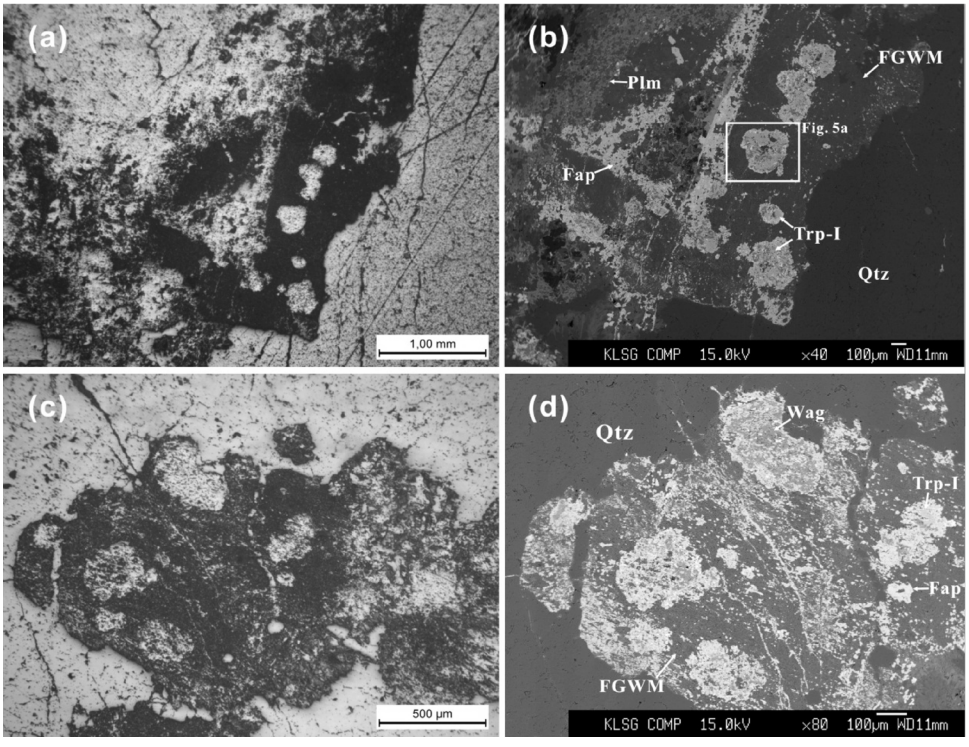

Fig. 2. Photomicrographs and backscattered-electron (BSE) images of the triphylite-I (sample NP-36, zone III) in fine-grained white muscovite interstitial to quartz. (a, b) Triphylite-I grains associated with palermoite, lazulite, fluorapatite, *etc*. (c, d) Triphylite-I grains associated with wagnerite and fluorapatite. Abbr.: Trp-I – triphylite-I, Fap – fluorapatite, Wag – wagnerite, Plm – palermoite, Qtz – quartz, FGWM – fine-grained white mica.

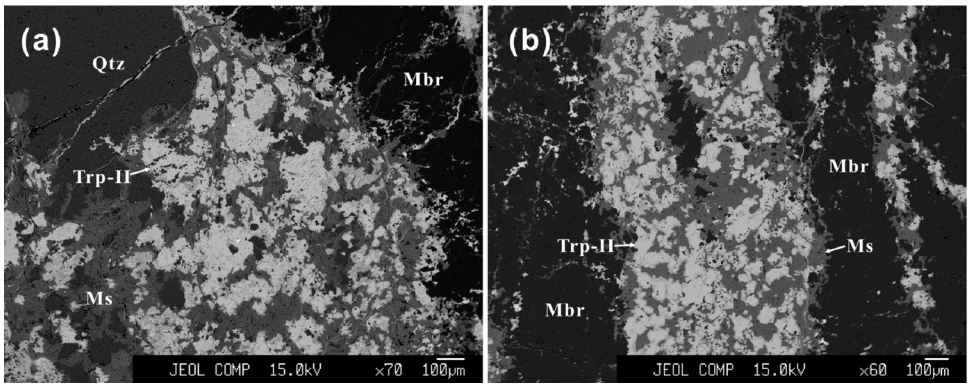

Fig. 3. BSE images of the triphylite-II assemblages. (a) Triphylite-II + fine-grained white muscovite assemblages between quartz and montebrasite (sample NP-30, zone IV). (b) Triphylite -II + narrow muscovite veins in montebrasite (sample NP-2, zone IV). Abbr.: Trp-II – triphylite-II, Mbr – montebrasite, Qtz – quartz, Ms – muscovite.

hydroxylapatite, fluorapatite, ludlamite, and anapaite are observed in this type of triphylite assemblages.

Electron-microprobe analyses indicate variable contents of FeO, MnO and MgO for the two types of triphylite (Table 1). Triphylite-I has slightly lower Fe and Mn contents (average 31.51 wt% FeO and 3.99 wt% MnO), but higher Mg contents (7.21 wt% MgO) than those of triphylite-II, with average values of 35.36 wt% FeO, 8.22 wt% MnO, and 0.46 wt% MgO. Figure 4 shows the different chemical compositions for triphylite-I and triphylite-II in the Mg–Fe_{tot}–Mn ternary diagram. The Fe/(Fe + Mn) ratio of triphylite-I (average 0.89) is significantly higher than that of triphylite-II (average 0.81) (Table 1).

4.2. Assemblages replacing triphylite-I: lazulite–wagnerite–fluorarrojadite-(BaNa)–fluorapatite

Globular grains of triphylite-I, included in fine-grained white mica from zones III and IV, are replaced by lazulite,

Table 1. Electron-microprobe analyses of triphylite from the Nanping No. 31 pegmatite dyke.

Occurrence	Trp-I				Trp-II			
	Zone III	Zone IV			Zone IV			
Sample	NP-36	NP-88	NP-101	Average (n = 9)	NP-2	NP-30	NP-65	Average (n = 23)
No.	1	1	2		2	4	2	
P_2O_5 (wt %)	47.04	46.96	46.03	47.22 (0.55)	46.68	46.95	46.22	46.14 (0.71)
SiO_2	0.01	0.02	0.02	0.03 (0.04)	–	0.02	–	0.01 (0.01)
Al_2O_3	0.00	0.00	0.01	0.02 (0.02)	0.02	0.02	0.04	0.01 (0.01)
FeO	32.38	31.24	30.24	31.51 (1.28)	36.70	33.50	35.75	35.36 (1.27)
MnO	3.06	3.53	5.43	3.99 (0.90)	6.28	8.42	7.81	8.22 (0.68)
MgO	7.16	7.17	8.38	7.21 (0.73)	0.35	0.58	0.36	0.46 (0.11)
CaO	0.08	0.07	–	0.09 (0.11)	–	0.06	–	0.09 (0.10)
Na_2O	–	–	–	0.01 (0.01)	–	0.08	0.04	0.02 (0.03)
K_2O	0.02	0.01	0.01	0.01 (0.01)	–	0.03	0.02	0.01 (0.01)
Li_2O*	9.90	9.89	9.69	9.94 (0.12)	9.82	9.88	9.73	9.71 (0.15)
Total	99.64	98.88	99.80	100.06	99.84	99.54	99.96	100.03
Structural formula calculated on the basis of P + Si = 1								
P (*apfu*)	1.000	0.999	1.000	0.999	1.000	1.000	1.000	1.000
Si	0.000	0.001	0.000	0.001		0.000		0.000
Al	0.000	0.000	0.000	0.000	0.001	0.000	0.001	0.000
Fe^{2+}	0.680	0.657	0.649	0.659	0.777	0.705	0.765	0.758
Mn	0.065	0.075	0.118	0.085	0.135	0.179	0.169	0.178
Mg	0.268	0.269	0.320	0.269	0.013	0.022	0.014	0.017
Ca	0.002	0.002		0.002		0.002		0.002
Na				0.000		0.004	0.002	0.001
K	0.001	0.000	0.000	0.000		0.001	0.001	0.000
Li	1.000	1.000	1.000	1.000	1.000	1.000	1.000	1.000
Fe/(Fe + Mn)	0.91	0.90	0.85	0.89	0.85	0.80	0.82	0.81

*: Li_2O was calculated based on stoichiometry; FeO as the total Fe; –: below the detection limits.

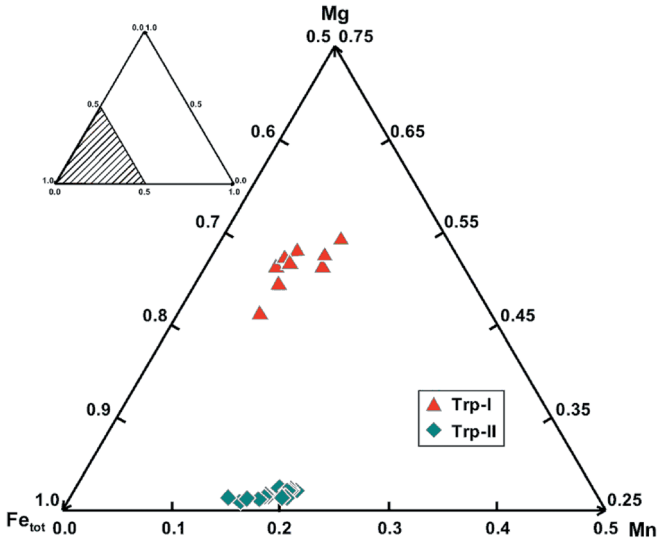

Fig. 4. Triangular Mg – Fe_{tot} – Mn diagram showing the compositional variations for triphylite-I and triphylite-II.

wagnerite, fluorarrojadite-(BaNa) and fluorapatite. In zone III, triphylite-I is successively replaced by lazulite, wagnerite, fluorarrojadite-(BaNa) and fluorapatite. Figure 5a shows the general paragenetic sequence of these phosphates. Lazulite occurs as anhedral grains or veinlets along fractures in the central portion of the granular aggregates of triphylite-I. The rim of these grains (less than 30 μm in width) is discontinuously composed of wagnerite and fluorapatite. Wagnerite is also distributed along the fractures of triphylite-I. Fluorarrojadite-(BaNa) forms anhedral grains, sporadically occurring along the rim and within the fractures of triphylite-I. In zone IV, triphylite-I was mainly replaced by wagnerite, fluorarrojadite-(BaNa) and fluorapatite (Fig. 5b). Wagnerite occurs as irregular aggregates (up to 25 μm across) in the fractures of triphylite-I. Fluorapatite mainly surrounds triphylite-I grains, and fluorarrojadite-(BaNa) is sporadically distributed in these assemblages.

Electron-microprobe analyses of these phosphate minerals yielded various compositional characteristics (Table 2). Lazulite shows a significant FeO content of 4.10 wt%, indicating a solid solution towards scorzalite (18 mol% scorzalite). Wagnerite contains 11.99 wt% FeO and 4.20 wt% MnO, as well as small amounts of OH, thus indicating a partial substitution towards triploidite, $(Mn,Fe)_2(PO_4)OH$, and wolfeite, $(Fe,Mn)_2(PO_4)OH$. The arrojadite-group mineral shows an enrichment in Ba and Na; its empirical formula is $(Ba_{0.58}Sr_{0.31}Na_{0.07}K_{0.04})_{\Sigma 1.00}Na_{2.00}(Ca_{0.71}Na_{2.07})_{\Sigma 2.78}(Fe^{2+}_{7.01}Mg_{3.89}Mn_{2.28})_{\Sigma 13.18}Al_{1.00}(PO_4)_{11}(PO_3OH)_{0.99}(F_{1.17}OH_{0.83})_{\Sigma 2.00}$, thus indicating that it corresponds to fluorarrojadite-(BaNa) (Chopin *et al*., 2006). Apatite-group minerals in this type of assemblages contain 3.17 wt% F, indicating that they correspond to fluorapatite. It is noteworthy that this fluorapatite also contains significant amounts of Mn (1.25 wt% MnO), Fe (0.51 wt% FeO), Mg (0.14 wt% MgO), Sr (0.44 wt% SrO), and Ba (0.13 wt% BaO) (Table 2).

4.3. Assemblages replacing triphylite-II

Triphylite-II in zone IV shows three distinct types of alteration assemblages involving fluorapatite, ludlamite and anapaite, respectively, as described below.

4.3.1. Fluorapatite aggregate

Secondary apatite-group minerals are extensively distributed in the Nanping No. 31 pegmatite zones. Fluorapatite was observed as one of the alteration products of triphylite-II in zone IV (Fig. 6a-b). In these replacement textures, triphylite-II is distributed in interstices of montebrasite and/or quartz, in close association with quartz and fine-grained muscovite. Fluorapatite forms irregular aggregates, mainly distributed in the central portion of triphylite-II crystals (Fig. 6a). A few remnants of triphylite, up to 5 μm across, are observed in the fluorapatite aggregates (Fig. 6b). Electron-microprobe analyses indicate that this phosphate, with an average content of 2.86 wt% F, corresponds to fluorapatite. It also shows a slight enrichment in

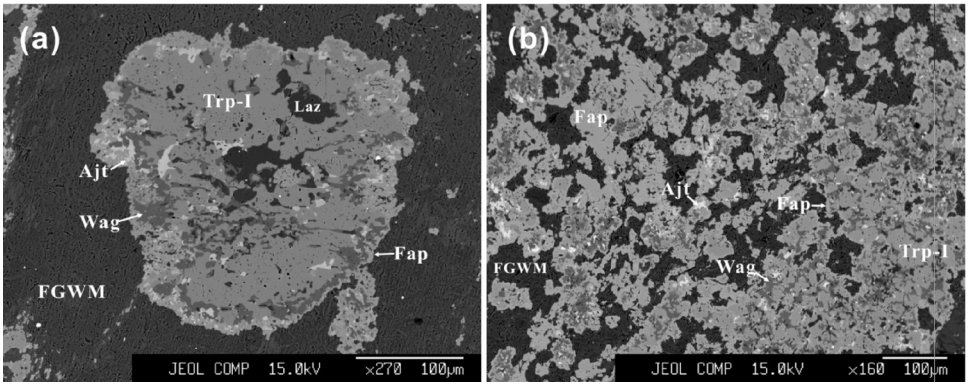

Fig. 5. (a) Triphylite-I replaced by wagnerite, lazulite, fluorarrojadite-(BaNa), and fluorapatite (sample NP-36, zone III). (b) Triphylite-I altered to wagnerite, fluorarrojadite-(BaNa), and fluorapatite (sample NP-88, zone IV). Abbr.: Trp-I – triphylite-I, Wag – wagnerite; Laz – lazulite; Ajt – fluorarrojadite-(BaNa), Fap – fluorapatite, FGWM – fine-grained white mica.

Table 2. Electron-microprobe analyses of phosphates associated with triphylite-I.

Mineral	Lazulite	Wagnerite	Fluorarrojadite-(BaNa)	Fluorapatite
Average (n =)	2	8	12	4
P_2O_5 (wt%)	45.00 (0.15)	40.24 (1.05)	42.34 (0.63)	40.86 (0.70)
SiO_2	0.09 (0.01)	0.09 (0.13)	0.02 (0.02)	0.07 (0.09)
Al_2O_3	33.25 (0.46)	0.05 (0.12)	2.54 (0.05)	0.07 (0.08)
FeO	4.10 (0.01)	11.99 (1.58)	25.01 (0.79)	0.51 (0.44)
MnO	0.07 (0.05)	4.20 (0.64)	8.03 (1.23)	1.25 (0.79)
MgO	11.51(0.36)	37.24 (1.50)	7.80 (1.06)	0.14 (0.24)
CaO	0.03 (0.02)	0.16 (0.07)	2.02 (0.19)	53.66 (0.90)
SrO	0.00 (0.01)	0.01 (0.01)	1.62 (1.16)	0.44 (0.12)
BaO	–	0.02 (0.05)	4.43 (1.83)	0.13 (0.12)
Na_2O	–	0.01 (0.01)	6.39 (0.33)	0.01 (0.02)
K_2O	0.01 (0.01)	0.01 (0.01)	0.09 (0.02)	0.08 (0.06)
F	–	10.49 (0.30)	1.10 (0.11)	3.17 (0.26)
H_2O	5.72 (0.02)	0.30 (0.20)	0.75 (0.10)	0.45 (0.27)
F = O		−4.40 (0.13)	−0.46 (0.03)	−1.33 (0.11)
Total	99.78	100.39	101.66	99.51
P (*apfu*)	1.995	0.997	11.993	2.994
Si	0.005	0.003	0.007	0.006
Al	2.052	0.002	1.002	0.007
Fe	0.180	0.294	7.006	0.037
Mn	0.003	0.104	2.275	0.092
Mg	0.899	1.627	3.891	0.019
Ca	0.001	0.005	0.714	4.914
Sr	0.000	0.000	0.312	0.022
Ba		0.000	0.583	0.004
Na		0.000	4.143	0.002
K	0.000	0.000	0.037	0.009
F		0.971	1.165	0.869
OH	1.000	0.029	0.835	0.131

Empirical formulae were calculated based on P + Si = 2, 1, 12, and 3 for lazulite, wagnerite, fluorarrojadite-(BaNa) and fluorapatite, respectively; FeO as the total Fe; –: below the detection limits; H_2O was calculated based on stoichiometry.

Mn (1.28 wt% MnO), Fe (0.73 wt% FeO), and Sr (0.16 wt% SrO) (Table 3).

4.3.2. Anapaite aggregate

Triphylite-II grains in zone IV are commonly replaced by anapaite (Fig. 6c), which forms small aggregates up to 30 μm across. These aggregates typically surround triphylite-II grains, or are distributed in the fractures of these grains. A few remnants of triphylite are present in the centre of anapaite aggregates. In some cases, triphylite-II grains are completely altered into anapaite. The chemical composition of anapaite was determined by electron microprobe (Table 3); the resulting empirical formula is $Ca_{2.00}(Fe^{2+}_{0.74}Mn_{0.20}Al_{0.02}Mg_{0.01})_{\Sigma 0.97}(PO_4)_2 \cdot 4H_2O$.

4.3.3. Ludlamite–anapaite assemblage

The alteration of triphylite-II crystals to ludlamite and anapaite was also observed (Fig. 6d). The assemblages are approximately 100–200 μm across. They usually keep the original outline of triphylite-II crystals. Figure 6d shows the general paragenetic sequence that exists among these phosphates: the triphylite grains were firstly replaced by ludlamite, and then by anapaite. A few remnants of triphylite are present in the anapaite and/or ludlamite aggregates.

Electron-microprobe analyses indicate that anapaite in this type of assemblage has slightly different CaO and FeO contents, compared to those of anapaite from the previous assemblage (Table 3). Ludlamite shows an empirical formula corresponding to $(Fe^{2+}_{2.55}Mn_{0.24}Mg_{0.01}Ca_{0.02})_{\Sigma 2.82}(PO_4)_2 \cdot 4H_2O$.

5. Discussion

5.1. The formation of triphylite in the Nanping No. 31 pegmatite

Triphylite is a lithium-iron phosphate mineral which was commonly reported as a primary (magmatic) phase in phosphate-bearing pegmatites and pegmatitic dykes (*e.g*., Shigley & Brown, 1985; Keller & Von Knorring, 1989; Roda *et al*., 2004; Vignola *et al*., 2008; Baijot *et al*., 2012; 2013). In the Nanping No. 31 pegmatite, however, triphylite occurs as small granular aggregates (Trp-1) in the fine-grained white micas from zones III and IV, and as veinlets or aggregates (Trp-2) in the fractures and rims of the primary montebrasite from zone IV (Figs. 2 and 3).

In zones III and IV, triphylite-I occurs as rounded grains in fine-grained muscovite (Figs. 2 and 5). Since triphylite-I

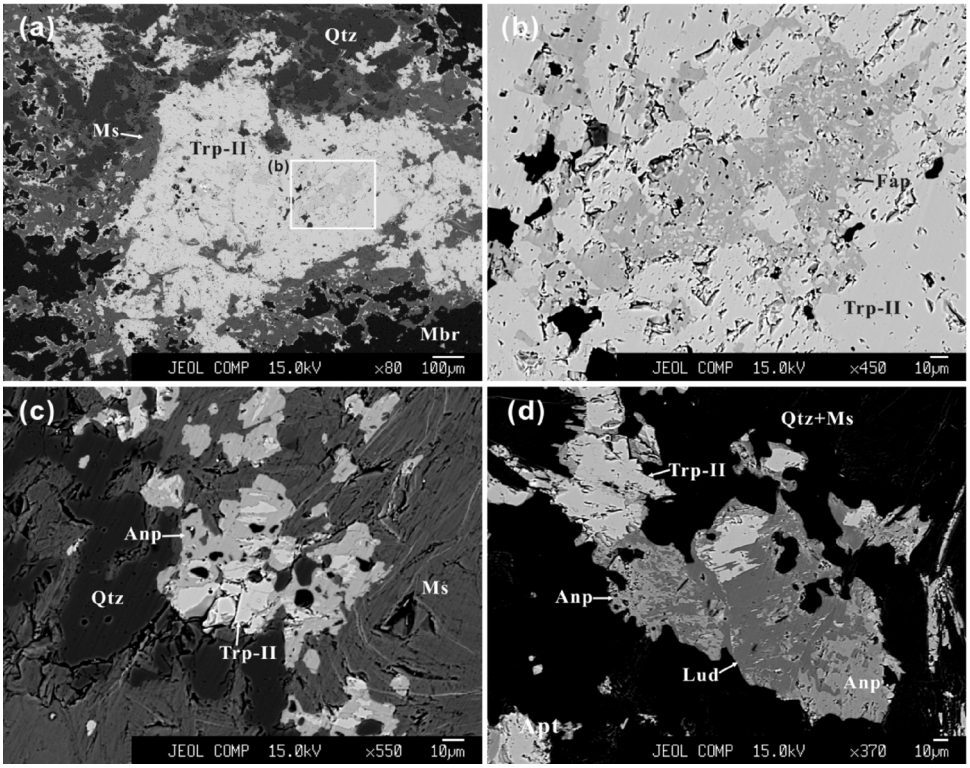

Fig. 6. BSE images of alteration assemblages of triphylite-II. (a, b) Triphylite-II altered to fluorapatite (sample NP-2, zone IV). (c) Triphylite-II replaced by anapaite (sample NP-30, zone IV). (d) Triphylite-II altered to ludlamite and anapaite (sample NP-30, zone IV). Abbr.: Trp-II – triphylite-II, Anp – anapaite, Lud – ludlamite, Fap – fluorapatite, Mbr – montebrasite, Qtz – quartz, Ms – muscovite.

grains show a rounded shape, and are optically oriented in the same direction, it seems obvious that they constitute relics of a previous, larger grain of primary triphylite. During the hydrothermal transformations affecting the pegmatite, this triphylite was transformed to muscovite; a similar transformation of spodumene to muscovite was previously reported by Rao *et al*. (2012) in the Nanping No. 31 pegmatite. Electron-microprobe analyses show that triphylite-I has high MgO content and a high Fe/(Fe + Mn) ratio (Table 1 and Fig. 4), thus confirming that triphylite-I crystallized during the early stages of magmatic differentiation. Indeed, the decrease of Mg and Fe contents of triphylite-type phosphates, during the pegmatite differentiation processes, has been widely described in the literature (Fransolet *et al*., 1985, 1985; Roda *et al*., 2004; Vignola *et al*., 2008; Baijot *et al*., 2012). Another argument, confirming the primary origin of triphylite-I, is the fact that triphylite-I from zone IV is enriched in Mn, compared to triphylite-I from zone III. This Mn enrichment follows the general trend of pegmatite differentiation (Ginzbourg, 1960).

Triphylite-II occurs as veinlets or aggregates in the fractures and rims of the primary montebrasite in zone IV (Fig. 3). Petrographic textures, with granular triphylite intimately intergrown with muscovite, indicate that the formation of triphylite-II is related to the hydrothermal transformation of the primary montebrasite in zone IV. Widespread hydrothermal alteration of primary minerals in this zone of the Nanping No. 31 pegmatite was documented in previous studies (Yang *et al*., 1994; 1995; Rao *et al*., 2009, 2011, 2012). Sharp contacts between the primary montebrasite and these secondary phases are considered to be typical textures of dissolution-reprecipitation processes (Putnis & Austrheim, 2010).

5.2. Hydrothermal transformation of triphylite in the Nanping No. 31 pegmatite

In granitic pegmatites, triphylite was commonly replaced by late hydrothermal or meteoric fluids, involving various metasomatic and/or dissolution-crystallization processes (Moore, 1973; Hawthorne, 1998). These metasomatic processes generate various mineral assemblages, which correspond to different transformation mechanisms (Keller & Von Knorring, 1989; Wise & Černý, 1990; Roda *et al*., 2004; Nizamoff, 2006; Vignola *et al*., 2011). In the present study, two types of triphylite, showing striking metasomatic processes induced by late hydrothermal fluids, are described (Figs. 4 and 5).

5.2.1. Hydrothermal transformation of triphylite-I: multiple replacements by late fluids

Triphylite-I in zones III and IV was replaced by lazulite, wagnerite, fluorarrojadite-(BaNa), and fluorapatite (Fig. 5). They display a general alteration sequence: triphylite-I → lazulite → wagnerite → fluorarrojadite-(BaNa) → fluorapatite, suggesting multiple alteration processes for triphylite. Lazulite aggregates or veinlets occurring in the central portion

Table 3. Electron-microprobe analyses of phosphates associated with triphylite-II.

Assemblage			Anapaite - ludlamite		
Mineral	Fluorapatite	Anapaite	Anapaite	Ludlamite	Primary montebrasite
Average (n =)	4	5	5	9	4
P_2O_5 (wt%)	41.99 (1.14)	35.94 (0.95)	35.94 (1.30)	33.40 (0.40)	50.56 (0.01)
SiO_2	0.01 (0.01)	0.01 (0.01)	0.03 (0.05)	0.00 (0.01)	0.01 (0.01)
Al_2O_3	0.02 (0.01)	0.22 (0.14)	0.79 (1.68)	0.02 (0.02)	32.90 (0.02)
FeO	0.73 (0.64)	13.43 (2.74)	15.83 (1.85)	43.06 (0.96)	0.11 (0.03)
MnO	1.28 (1.03)	3.52 (0.73)	3.32 (0.84)	3.92 (0.65)	0.03 (0.01)
MgO	0.01 (0.02)	0.11 (0.08)	0.06 (0.05)	0.11 (0.08)	0.00 (0.00)
CaO	53.62 (1.16)	28.77 (2.17)	25.91 (1.41)	0.29 (0.64)	0.02 (0.03)
SrO	0.16 (0.27)	0.18 (0.30)	0.03 (0.05)	0.00 (0.00)	0.00 (0.12)
BaO	0.03 (0.05)	0.13 (0.11)	0.11 (0.04)	0.06 (0.16)	0.13 (0.67)
Na_2O	0.01 (0.01)	0.04 (0.01)	0.04 (0.02)	0.01 (0.02)	0.01 (0.02)
K_2O	0.03 (0.03)	0.11 (0.09)	0.15 (0.30)	0.04 (0.02)	0.02 (0.87)
Li_2O*					10.64 (0.42)
F	2.86 (0.19)	0.05 (0.13)	–	0.02 (0.01)	0.55 (0.33)
H_2O	0.84 (0.25)	18.19 (0.45)	18.25 (0.63)	16.92 (0.21)	6.15 (0.34)
F = O	−1.20 (0.08)	−0.02 (0.05)		−0.01 (0.00)	−0.23 (0.87)
Total	100.39	100.69	100.45	97.86	100.92
P (*apfu*)	2.999	1.999	1.998	2.000	1.000
Si	0.001	0.001	0.002	0.000	0.000
Al	0.002	0.017	0.065	0.002	0.906
Fe	0.052	0.739	0.869	2.549	0.002
Mn	0.091	0.196	0.186	0.235	0.001
Mg	0.001	0.010	0.005	0.012	0.000
Ca	4.787	2.000	1.801	0.021	0.001
Sr	0.008	0.007	0.001	0.000	0.000
Ba	0.001	0.003	0.003	0.002	0.001
Na	0.002	0.005	0.005	0.002	0.001
K	0.003	0.010	0.013	0.004	0.001
Li					1.000
F	0.763	0.010	0.000	0.006	0.040
OH	0.237	3.990	4.000	3.994	0.960

Empirical formulae were calculated based on P + Si = 3, 2, 2, and 1 for fluorapatite, anapaite, ludiamite and montebrasite, respectively; *: Li_2O was calculated based on stoichiometry; FeO as the total Fe; –: below the detection limits; H_2O were calculated based on stoichiometry.

of triphylite-I suggest the alteration of triphylite-I first by Mg-rich fluids. Fransolet (1975) indicated that Al^{3+} was introduced from local muscovite for the formation of scorzalite—lazulite in this alteration process. The alteration of triphylite to lazulite, then to wagnerite, reflects the high activities of Mg and F in these early stage hydrothermal fluids. This feature is in good agreement with the results of the study of fluids inclusions in the Nanping pegmatite (Yang *et al*., 1994). In a second Na-stage, fluorarrojadite-(BaNa), which shows an average content of 6.39 wt% Na_2O, crystallized; this observation is in good agreement with the formation of arrojadite-group minerals during the albitization of K-feldspar (Malló *et al*., 1995). Finally, increasing activities of F and Ca in late fluids lead to the crystallization of fluorapatite, as already mentioned by Fransolet *et al*. (1985) and Smeds *et al*. (1998).

5.2.2. Hydrothermal transformation of triphylite-II: late Ca-metasomatism

Triphylite-II in zone IV is transformed into different mineral assemblages such as fluorapatite aggregates, anapaite aggregates, and ludlamite–anapaite assemblages (Fig. 6). Chemical features and paragenetic relationships indicate that late Ca-bearing fluids are responsible for the transformation of triphylite-II. Fluorapatite typically occurs in the central portion of triphylite-II (Fig. 6a, b), indicating that fluorapatite has grown at the expense of triphylite-II. The high F-content of this fluorapatite was likely derived from the alteration of the associated primary montebrasite, which shows 0.55 wt% F (Table 3). The low FeO and MnO contents indicate that large amounts of Fe and Mn were leached out by the Ca-rich fluids. Anapaite and ludlamite are commonly distributed along the rims and fractures of triphylite-II, indicating that they constitute relatively late transformation products of triphylite-II (Fig. 6c, d), compared to fluorapatite. The chemical analyses (Tables 1 and 3) allow us to propose the reaction $2LiFePO_4 + 2Ca^{2+} + 4H_2O \rightarrow Ca_2Fe(PO_4)_2{\cdot}4H_2O + Fe^{2+} + 2Li^+$, which expresses the direct conversion of triphylite-II to anapaite. The transformation of triphylite-II to ludlamite and anapaite may be described by the reaction $4LiFePO_4 + 2Ca^{2+} + 8H_2O \rightarrow Ca_2Fe(PO_4)_2{\cdot}4H_2O +$

$Fe_3(PO_4)_2{\cdot}4H_2O + 4Li^+$. These reactions indicate the alteration scheme of cationic exchange in combination with hydration (Nizamoff, 2006). Therefore, the high activity of Ca in the late fluids triggered the hydrothermal replacement of triphylite-II to fluorapatite, ludlamite and anapaite. Such Ca-rich hydrothermal fluids can also be found in other localities, *e.g*. in the Palermo #2 pegmatite, New Hampshire (Nizamoff, 2006).

6. Conclusions

(1) Two types of triphylite were distinguished in the Nanping No. 31 pegmatite. Triphylite-I occurs as rounded grains in fine grained white mica from zones III and IV; it was formed during a primary magmatic stage. Triphylite-II is related to the hydrothermal transformation of the primary montebrasite in zone IV.
(2) The two types of triphylite exhibit various metasomatic alteration phenomena. Different assemblages of secondary minerals reveal different metasomatic transformation mechanisms of triphylite, which took place at different stages of pegmatite evolution.
(3) Triphylite-I from zones III and IV shows multiple hydrothermal transformations: triphylite-I → lazulite → wagnerite → fluorarrojadite-(BaNa) → fluorapatite, suggesting successive replacement processes during Mg-rich, Na-rich, and Ca-rich hydrothermal stages. Triphylite-II is mainly replaced by fluorapatite, anapaite and ludlamite; these replacement processes result from cationic exchanges in combination with hydration, due to the presence of Ca-bearing fluids.

Acknowledgements: Financial support for the research was provided by NSF of China [Grant No. 41102020] and by the Fundamental Research Funds for the Central Universities.

References

Baijot, M., Hatert, F., Philippo, S. (2012): Mineralogy and geochemistry of phosphates and silicates in the Sapucaia pegmatite, Minas Gerais, Brazil: genetic implications. *Can. Mineral.*, **50**, 1531–1554.

Baijot, M., Hatert, F., Philippo, S., Dal Bo, F. (2013): The phosphate mineral assemblages from Jocão pegmatite, Minas Gerais, Brazil. *Can. Mineral.*, **in press**.

Černý, P. (1991): Rare-element granitic pegmatites. Part I: anatomy and internal evolution of pegmatite deposits. *Geosci. Can.*, **18**, 49–67.

Černý, P. & Ercit, T.S. (2005): The classification of granitic pegmatites revisited. *Can. Mineral.*, **40**, 2005–2026.

Chopin, C., Oberti, R., Cámara, F. (2006): The arrojadite enigma. II. Compositional space, new members, and nomenclature of the group. *Am. Mineral.*, **91**, 1260–1270.

Dokko, K., Koizumi, S., Nakanob, H., Kanamura, K. (2007): Particle morphology, crystal orientation, and electrochemical reactivity of $LiFePO_4$ synthesized by the hydrothermal method at 443 K. *J. Mater. Chem.*, **17**, 4803–4810.

Fransolet, A.M. (1975): On scorzalite from the Angarf-Sud pegmatite, Zenaga Plain, Anti-Atlas, Morocco. *Fortschritte Der Mineralogie*, **52**, 285–291.

Fransolet, A.-M., Abraham, K., Speetjens, J.-M. (1985): Evolution génétique et signification des associations de phosphates de la pegmatite d'Angarf-Sud, plaine de Tazenakht, Anti-Atlas, Maroc. *Bull. Minéral.*, **108**, 551–574.

Fransolet, A.M., Keller, P., Fontan, F. (1986): The phosphate mineral associations of the Tsaobismund pegmatite, Namibia. *Contrib. Mineral. Petrol.*, **92**, 502–517.

Hatert, F., Ottolini, L., Schmid-Beurmann, P. (2011): Experimental investigation of the alluaudite + triphylite assemblage, and development of the Na-in-triphylite geothermometer: applications to natural pegmatite phosphates. *Contrib. Mineral. Petrol.*, **161**, 531–546.

Hawthorne, F.C. (1998): Structure and chemistry of phosphate minerals. *Mineral. Mag.*, **62**, 141–164.

Keller, P. & Von Knorring, O. (1989): Pegmatites at the Okatjimukuju farm, Karibib, Namibia Part I: Phosphate mineral associations of the Clementine II pegmatite. *Eur. J. Mineral.*, **1**, 567–593.

Li, Z.L., Zhang, J.Z., Wu, Q.H., Ouyang, Z.H. (1983): Geological and geochemical characteristics of a certain pegmatite ore field of rare metals in Fujian Province. *Mineral Deposits*, **2**(2), 49–58. (in Chinese with English abstract)

London, D. (2008): *Pegmatites*. *The Can. Mineral. Spec. Publ.*, **10**, 347 p.

Malló, A., Fontan, F., Melgarejo, J.-C., Mata, J.M. (1995): The Albera zoned pegmatite field, Eastern Pyrenees, France. *Mineral. Petrol.*, **55**, 103–116.

Moore, P.B. (1973): Pegmatite phosphates: descriptive mineralogy and crystal chemistry. *Mineral. Rec.*, **4**, 103–130.

Nizamoff, J. (2006): The mineralogy, geochemistry and phosphate paragenesis of the Palermo #2 Pegmatite, North Groton, New Hampshire. University of New Orleans, Unpublished Master Thesis.

Padhi, A.K., Nanjundaswamy, K.S., Goodenough, J.B. (1997): Phosphoolivines as positive materials for rechargeable lithium batteries. *J. Electrochem. Soc.*, **144**, 1188–1194.

Putnis, A. & Austrheim, H. (2010): Fluid-induced processes: metasomatism and metamorphism. *Geofluids*, **10**, 254–269.

Rao, C., Wang, R.C., Hu, H., Zhang, W.L. (2009): Complex internal texture in oxide minerals from the Nanping No. 31 dyke of granitic pegmatite, Fujian Province, southeastern China. *Can. Mineral.*, **47**, 1195–1212.

Rao, C., Wang, R.C., Hu, H. (2011): Paragenetic assemblages of beryllium silicates and phosphates from the Nanping no. 31 granitic pegmatite dyke, Fujian province, southeastern china. *Can. Mineral.*, **49**, 1175–1187.

Rao, C., Wang, R.C., Zhang, A.C., Hu, H. (2012): The corundum + tourmaline nodules related to hydrothermal alteration of spodumene in the Nanping No. 31 pegmatite dyke, Fujian province, southeastern China. *Can. Mineral.*, **50**, 1623–1635.

Rao, C., Wang, R., Hatert, F., Gu, X., Ottolini, L., Hu, H., Dong, C., Dal Bo, F., Baijot, M. (2013): Strontiohurlbutite, $SrBe_2(PO_4)_2$, a new mineral from Nanping No. 31 pegmatite, Fujian Province, Southeastern China. *Am. Mineral.*, **in press**.

Roda, E., Pesquera, A., Fontan, F., Keller, P. (2004): Phosphate mineral associations in the Canada pegmatite (Salamanca, Spain): paragenetic relationships, chemical compositions, and implications for pegmatite evolution. *Am. Mineral.*, **89**, 110–125.

Shigley, J.E. & Brown, G.E. (1985): Occurrence and alteration of phosphate minerals at the Stewart Pegmatite, Pala District, San Diego County, California. *Am. Mineral.*, **70**, 395–408.

Simmons, W., Webber, K.L., Falster, A.U., Nizamoff, J.W. (2003): *Pegmatology*. Rubellite Press, New Orleans, 176 p.

Smeds, S.-A., Uher, P., Černý, P., Wise, M.A., Gustafsson, L., Penner, P. (1998): Graftonite – beusite in Sweden: primary phases, products of exsolution, and distribution in zoned populations of granitic pegmatites. *Can. Mineral.*, **36**, 377–394.

Vignola, P., Diella, V., Oppizzi, P., Tiepolo, M., Weiss, S. (2008): Phosphate assemblages from the Brissago granitic pegmatite, Western Southern Alps, Switzerland. *Can. Mineral.*, **46**, 635–650.

Vignola, P., Diella, V., Ferrari, E.S., Fransolet, A.M. (2011): Complex mechanisms of alteration in a graftonite + sarcopside + triphylite association from the Luna pegmatite, Piona, Lecco province, Italy. *Can. Mineral.*, **49**, 765–776.

Wise, M.A. & Černý, P. (1990): Beusite-triphylite intergrowths from the Yellowknife pegmatite field, Northwest Territories. *Can. Mineral*, **28**, 133–139.

Yang, Y.Q., Ni, Y.X., Guo, Y.Q., Qiu, N.M., Chen, C.H., Cai, C.F., Zhang, Y.P., Liu, J.B., Chen, Y.X. (1987): Rock-forming and ore-forming characteristics of the Xikeng granitic pegmatites in Fujian Province. *Mineral. Deposits.*, **6**, 10–21. (in Chinese with English abstract)

Yang, Y.Q., Wang, W.Y., Ni, Y.X., Chen, C.H., Zhu, J.H. (1994): Phosphate minerals and their geochemical evolution of granitic pegmatite in Nanping, Fujian Province. *Geol. Fujian*, **13**, 215–226. (in Chinese with English abstract)

Yang, Y.Q., Wang, W.Y., Ni, Y.X., Chen, C.H., Zhu, J.H. (1995): A study on montebrasite in Nanping granitic pegmatite. *Geol. Fujian*, **14**, 8–21. (in Chinese with English abstract)

Zhao, T., Chu, W.S., Zhao, H.F., Liang, X.Q., Xu, W., Yu, M.J., Xia, D.G., Wu, Z.Y. (2010): XAS study of $LiFePO_4$ synthesized by solid state reactions and hydrothermal method. *Nucl. Instrum. Methods Phys. Res., Sect. A.*, **619**, 122–127.

Received 17 May 2013
Modified version received 25 September 2013
Accepted 18 October 2013